

Optical enhanced interferometry with two-mode squeezed twin-Fock states and parity detection*

Li-Li Hou(侯丽丽)¹, Shuai Wang(王帅)^{1,†}, and Xue-Fen Xu(许雪芬)^{2,‡}

¹*School of Mathematics and Physics, Jiangsu University of Technology, Changzhou 213001, China*

²*Department of Fundamental Courses, Wuxi Institute of Technology, Wuxi 214121, China*

(Received 11 September 2019; revised manuscript received 30 November 2019; accepted manuscript online 7 January 2020)

We theoretically investigate the quantum enhanced metrology using two-mode squeezed twin-Fock states and parity detection. Our results indicate that, for a given initial squeezing parameter, compared with the two-mode squeezed vacuum state, both phase sensitivity and resolution can be enhanced when the two-mode squeezed twin-Fock state is considered as an input state of a Mach-Zehnder interferometer. Within a constraint on the total photon number, although the two-mode squeezed vacuum state gives the better phase sensitivity when the phase shift φ to be estimated approaches to zero, the phase sensitivity offered by these non-Gaussian entangled Gaussian states is relatively stable with respect to the phase shift itself. When the phase shift slightly deviates from $\varphi = 0$, the phase sensitivity can be still enhanced by the two-mode squeezed twin-Fock state over a broad range of the total mean photon number where the phase uncertainty is still below the quantum standard noise limit. Finally, we numerically prove that the quantum Cramér-Rao bound can be approached with the parity detection.

Keywords: quantum optics, phase sensitivity, quantum metrology

PACS: 42.50.Dv, 03.65.Ta

DOI: 10.1088/1674-1056/ab6837

1. Introduction

Optical interferometers are important devices in quantum metrology. Mach-Zehnder interferometers (MZIs) and SU(1,1) interferometers^[1–6] are two kinds of basic optical interferometers, which are widely used to measure an unknown phase shift in the two arms of an interferometer and its phase sensitivity $\Delta\varphi$. In general, the precision of phase estimation within these settings crucially depends on the input states as well as the detection schemes. It is well known that nonclassical quantum states, such as the squeezed state and the Fock state, are the most key resources to improve the precision of phase estimation in an interferometer. In a lossless MZI, a few decades ago Caves^[2] demonstrated that the sensitivity of phase estimation using the coherent light together with the squeezed vacuum one could beat the standard quantum noise limit (SNL), namely, $\Delta\varphi = 1/\sqrt{\bar{n}}$, where \bar{n} is the total photon number of input states. Actually, the so-called Heisenberg limit (HL),^[7,8] $\Delta\varphi = 1/\bar{n}$, can also be achieved when the coherent light and the squeezed vacuum one are mixed in roughly equal intensities.^[5,6]

In recent years, many other nonclassical states have been studied to improve the precision of phase estimation based on an MZI.^[9–18] For example, an MZI with the NOON state can offer the HL limit in principle.^[9,10] Unfortunately, ideal NOON states are challenged to generate in experiments and these states are extremely fragile.^[11,12] Another way to ap-

proach the HL limit is through the injection of the twin-Fock state $|n, n\rangle$ into the first beam splitter of an MZI.^[13] Compared with the NOON state, the twin-Fock state is easier to generate and more robust against photon loss.^[6,14–17] Therefore, the twin-Fock state is traditionally used to approximate the NOON state. Especially, in the case of the input twin-Fock state $|n, n\rangle$ with two photons ($n = 1$), the state inside the interferometer after the first beam splitter is just a NOON state. In addition, it has been proved that the twin-Fock state with six photons can be prepared in experiments using photon pairs from spontaneous parametric down conversion.^[15,16] As continuous-variable superpositions of twin-Fock states, it is found that an MZI with a two-mode squeezed vacuum state (TMSVS) and parity detection can offer the sub-Heisenberg sensitivity.^[19] However, it is difficult to prepare these Gaussian entangled states with a large mean photon number. In experiments, the largest achievable total photon number of the TMSVS so far is about 4 in a stable optical configuration, and the corresponding squeezing parameter is about $r \approx 1.15$ (i.e., about 10 dB).^[20] On the other hand, Gerry and Mimih^[21] showed that the phase sensitivity for these entangled Gaussian states is very unstable with respect to the phase shift itself. When the phase shift moderately deviates from the optimal values of the phase shift (for example, $\varphi = 0$), the phase sensitivity will rapidly becomes worse, even above the SNL. To remedy these problems, the non-Gaussian entangled states, such as photon-subtracted

*Project supported by the National Natural Science Foundation of China (Grant No. 11404040) and Qing Lan Project of the Higher Educations of Jiangsu Province of China.

†Corresponding author. E-mail: wshslxy@jsut.edu.cn

‡Corresponding author. E-mail: xuxf@wxit.edu.cn

TMSVS^[22,23] and photon-added TMSVS,^[24] have been used to improve the precision of phase estimation based on an MZI with parity detection.

Besides the photon-subtracted or photon-added TMSVS, two-mode squeezed number states are also a broad and meaningful class of continuous-variable non-Gaussian entangled states. Such states were originally introduced by Chizhow,^[25] where the photon number statistics and the phase properties have been investigated. The analysis of their inseparabilities was also carried out via the Neumann entropy.^[26,27] It has shown that, for a given initial squeezing, the two-mode squeezed number state with a higher number state has a larger amount of entanglement. Very recently, non-Gaussianity dynamics of such states has also been studied.^[28] In this work, we investigate the applications of the two-mode squeezed number states on the quantum enhanced metrology. In many applications, pair creation occurs starting from the vacuum. Therefore, here we mainly consider the two-mode squeezed twin-Fock state (TMSTFS) as the input state of an MZI, and investigate the performance of the TMSTFS on phase estimation via both quantum Fisher information and parity detection. Theoretically, a TMSTFS is obtained by applying a two-mode squeezed operator $S_2(\xi) = \exp[\xi \hat{a}^\dagger \hat{b}^\dagger - \xi^* \hat{a} \hat{b}]$ with $\xi = re^{i\theta}$ to a twin-Fock state, which is given by^[25]

$$|\text{TMSTFS}\rangle = S_2(\xi) |n, n\rangle, \quad (1)$$

with the total mean photon number

$$\bar{N} = 2n \cosh(2r) + 2 \sinh^2 r. \quad (2)$$

Obviously, for a given squeezing parameter r , the total photon number increases with the value of the n . Mathematically, the scenario under our consideration covers two special cases of significance. (i) When $n = 0$, $|\text{TMSTFS}\rangle$ is a TMSVS, and it reduces to the input state in Ref. [19]. (ii) When $r = 0$, $|\text{TMSTFS}\rangle$ is a twin-Fock state, and the applications of this state in quantum metrology have been considered in Refs. [7,13].

The remainder of this paper is organized as follows. Section 2 introduces a brief review about the TMSTFS, as well as their entanglement. In Section 3, we study the quantum Fisher information F_Q of the TMSTFS and the quantum Cramér–Rao bound (QCRB). In Section 4, we present the parity-based phase estimation scheme with calculations of its signal and phase sensitivity. Our results show that the phase sensitivity for these non-Gaussian entangled Gaussian states is relatively stable with respect to the phase shift itself. The QCRB expressed by $\Delta\phi_{\min} = 1/\sqrt{F_Q}$ can also be reached by implementing the parity detection. Our main results are summarized in Section 5.

2. Two-mode squeezed twin-Fock and its entanglement

Following the work in Ref. [29], the TMSTFS can be considered as the TMSVS excited by the Laguerre polynomials operator, i.e.,

$$|\text{TMSTFS}\rangle = \frac{(-e^{-i\theta} \tanh r)^n}{\cosh r} L_n \left(\frac{2\hat{a}^\dagger \hat{b}^\dagger e^{i\theta}}{\sinh(2r)} \right) \times \exp[\hat{a}^\dagger \hat{b}^\dagger e^{i\theta} \tanh r] |0, 0\rangle, \quad (3)$$

where the generating function of L_n is

$$L_n(z, z^*) = \frac{(-1)^n \partial^{2n}}{n! \partial t^n \partial \tau^n} \exp[-t\tau + tz + \tau z^*] |_{t=\tau=0}. \quad (4)$$

Equation (3) indicates that the TMSTFS can be considered as a superposition of photon-added TMSVS.^[24]

Although entanglement is not a critical resource for quantum-enhanced metrology,^[30,31] entangled photon number states are indeed helpful for phase estimation.^[9,10,32] For our purpose, let us review the von Neumann entropy of the TMSTFS.^[27] For a pure state in the Schmidt decomposed form, the quantum entanglement is characterized by the partial von Neumann entropy.^[33] Based on Eq. (3), the Schmidt decomposed form of the TMSTFS can be easily obtained, i.e.,

$$|\text{TMSTFS}\rangle = \sum_{m=0}^{\infty} C_m(n, r) |m, m\rangle, \quad (5)$$

where the Schmidt coefficient C_m is given by^[25]

$$C_m(n, r) = \sum_{k=0}^{\min[m, n]} \frac{(-1)^{n-k} m! n! \sinh^{-2k} r}{(k!)^2 (m-k)! (n-k)!} \times \frac{\tanh^{m+n} r}{\cosh r} e^{i(m-n)\theta}. \quad (6)$$

Similar to the TMSVS, the TMSTFS also remains a superposition of twin-Fock states. From Eq. (5), the von Neumann entropy of the TMSTFS can be directly obtained,^[27]

$$E(|\text{TMSTFS}\rangle) = \sum_{m=0}^{\infty} |C_m|^2 \log_2 |C_m|^2. \quad (7)$$

In the case of $n = 0$, equation (7) reduces to $E = \cosh^2 r \log_2(\cosh^2 r) - \sinh^2 r \log_2(\sinh^2 r)$, the amount of the entanglement of the TMSVS. For the TMSTFS with different values of n , it can be evaluated numerically by their Schmidt coefficients. As pointed out in Ref. [27], the entanglement of the TMSTFS becomes larger when the value of n increases for a fixed value of squeezing parameter r as shown in Fig. 1(a). This may be because the TMSTFS contains more photons with the increase of n as indicated by Eq. (2). On the other hand, it may be interesting to investigate whether or not the TMSTFS holds the larger entanglement than the TMSVS within a constraint on the total mean photon number. From Fig. 1(b), we can clearly see that, for a fixed total mean photon number, the TMSVS holds the larger entanglement in this scenario than the TMSTFS.

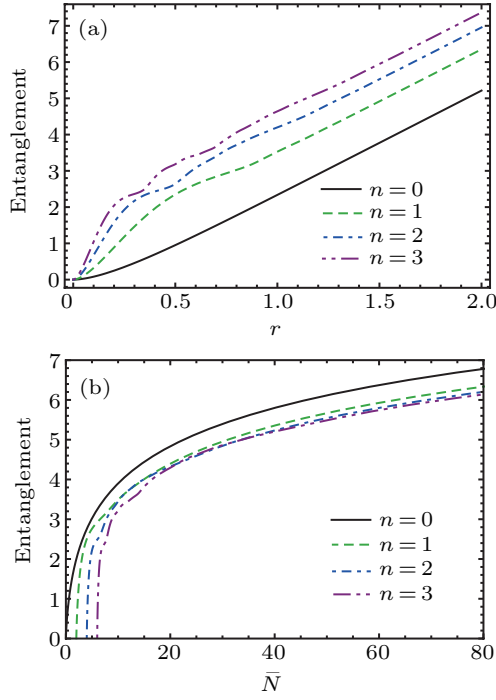


Fig. 1. Entanglement entropy of the TMSTFS with some different values of n . (a) Entanglement entropy as a function of the squeezing parameter r . (b) Entanglement entropy as a function of the total mean photon number.

3. Quantum Cramér–Rao bound

Here we consider an balanced MZI interferometer whose two input ports are fed by the TMSTFS as shown in Fig. 2. For such an interferometer, it is mainly composed of two beam splitters and two phase shifters. Then, according to the work in Ref. [1], the unitary transformation operator associated with such a balanced MZI can be written as

$$\hat{U}(\varphi) = e^{i\frac{\pi}{2}\hat{J}_1} e^{-i\varphi\hat{J}_3} e^{-i\frac{\pi}{2}\hat{J}_1} = e^{-i\varphi\hat{J}_2}, \quad (8)$$

where φ is the unknown phase shift between the two modes of the MZI to be estimated. Those angular momentum operators in Eq. (8) can be expressed in terms of two sets of Bosonic operators,

$$\begin{aligned} \hat{J}_1 &= \frac{1}{2}(\hat{a}^\dagger\hat{b} + \hat{a}\hat{b}^\dagger), & \hat{J}_2 &= \frac{1}{2i}(\hat{a}^\dagger\hat{b} - \hat{a}\hat{b}^\dagger), \\ \hat{J}_3 &= \frac{1}{2}(\hat{a}^\dagger\hat{a} - \hat{b}^\dagger\hat{b}). \end{aligned} \quad (9)$$

They satisfy the commutation relation $[\hat{J}_i, \hat{J}_j] = i\epsilon_{ijk}\hat{J}_k$ ($i, j, k = 1, 2, 3$) and commute with the Casimir operator $\hat{J}_0 = \frac{1}{2}(\hat{a}^\dagger\hat{a} + \hat{b}^\dagger\hat{b})$. Here \hat{a}^\dagger (\hat{b}^\dagger) and \hat{a} (\hat{b}) are the Bosonic creation (annihilation) operators in mode A (B) of the MZI, respectively. When a pure state propagates through such an MZI, the resulted output state is given by

$$|\text{out}\rangle_{\text{MZI}} = e^{-i\varphi\hat{J}_2} |\text{in}\rangle. \quad (10)$$

Applying the following unitary transformations

$$e^{-i\varphi\hat{J}_2}\hat{a}^\dagger e^{i\varphi\hat{J}_2} = \hat{a}^\dagger \cos \frac{\varphi}{2} + \hat{b}^\dagger \sin \frac{\varphi}{2},$$

$$e^{-i\varphi\hat{J}_2}\hat{b}^\dagger e^{i\varphi\hat{J}_2} = \hat{b}^\dagger \cos \frac{\varphi}{2} - \hat{a}^\dagger \sin \frac{\varphi}{2}, \quad (11)$$

and the relation $e^{-i\varphi\hat{J}_2} |0\rangle_a |0\rangle_b = |0\rangle_a |0\rangle_b$, in general, one can derive the explicit form of the output state of the MZI.

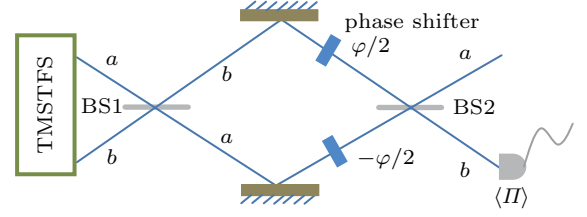


Fig. 2. The Mach–Zehnder interferometer used for the detection of the phase shift when the TMSTFS is injected into the first beam splitter.

In this section, we investigate the QCRB, which gives an ultimate limit to the precision of phase sensitivity for all possible locally unbiased estimators and the most general measurements, which is expressed by the quantum Fisher information,^[34] i.e.,

$$\Delta\varphi_{\text{QCRB}} = \frac{1}{\sqrt{F_Q}}. \quad (12)$$

For a pure state considered as an input state of the MZI, the quantum Fisher information F_Q simply reads^[35]

$$F_Q = 4 \left[\langle \text{in} | \hat{J}_2^2 | \text{in} \rangle - |\langle \text{in} | \hat{J}_2 | \text{in} \rangle|^2 \right]. \quad (13)$$

Therefore, for the TMSTFS as an interferometer input state, we derive the quantum Fisher information as follows:

$$F_Q = (2 + 3 \sinh^2(2r)) (n + n^2) + \sinh^2(2r). \quad (14)$$

On the other hand, in terms of the total mean photon number \bar{N} , equation (14) can also be rewritten as

$$F_Q = \frac{3}{4}\bar{N}^2 + \frac{1}{4} \left(\frac{\bar{N} + 1}{2n + 1} \right)^2 + \frac{3}{2}\bar{N} - \left(n^2 + n + \frac{1}{4} \right). \quad (15)$$

Based on Eqs. (12) and (14), one can clearly see that the QCRB can be enhanced by increasing the values of n for a given initial squeezing parameter r . Thus, the TMSTFS indeed can give the better phase sensitivity. On the other hand, based on Eqs. (12) and (15), we can also see that, within a constraint on the total mean photon number, the TMSVS gives the higher phase sensitivity. In addition, one can see from Eqs. (12), (14), and (15) that the properties of the QCRB offered by the TMSTFS are similar to that of its entanglement.

4. Parity detection on an MZI interferometer

In the above discussion, we have investigated the phase sensitivity limit based on direct calculation of the quantum Fisher information. In the following, we show that the QCRB $\Delta\varphi_{\text{min}}$ can be reached with the parity detection in the case $\varphi \rightarrow 0$. Actually, for a certain type of path-symmetric states,

the detection of photon number parity can achieve the QCRB at particular values of phase shift φ .^[36] For the TMSTFS considered as an interferometer state, we can prove that both homodyne detection^[37–39] and intensity detection^[40–43] are not suitable for the phase estimation. Therefore, in the work we mainly consider the parity detection as our measuring scheme.

4.1. The signal of the parity detection

For the convenience of the calculation, it is useful to expand the TMSTFS in the basis of the coherent state,

$$\begin{aligned} |\text{TMSTFS}\rangle &= \frac{\tanh^n r}{\cosh r} \int \frac{d^2\alpha d^2\beta}{\pi^2} L_n \left(\frac{2\alpha^* \beta^*}{\sinh(2r)} \right) \\ &\times \exp \left[-\frac{1}{2} (|\alpha|^2 + |\beta|^2) \right. \\ &\left. + \alpha^* \beta^* \tanh r \right] |\alpha, \beta\rangle, \end{aligned} \quad (16)$$

where $|\alpha\rangle$ ($|\beta\rangle$) is a coherent state with complex quadrature amplitude α (β). Here, we have ignored the phase θ of the TMSTFS light, because this parameter has no effect on the phase estimation. From Eqs. (10), (11), and (16), when the TMSTFS propagates through the MZI, the resulted output state reads

$$\begin{aligned} |\text{out}\rangle_{\text{MZI}} &= \text{sechr} \frac{\partial^{2n}}{n! \partial x^n \partial y^n} \int \frac{d^2\alpha d^2\beta}{\pi^2} \\ &\times \exp \left[-|\alpha|^2 - |\beta|^2 + \alpha^* \beta^* \tanh r \right. \\ &\left. - xy \tanh r + \alpha^* x \text{sechr} + \beta^* y \text{sechr} \right] \\ &\times \exp \left[\left(\alpha \cos \frac{\varphi}{2} - \beta \sin \frac{\varphi}{2} \right) \hat{a}^\dagger \right. \\ &\left. + \left(\alpha \sin \frac{\varphi}{2} + \beta \cos \frac{\varphi}{2} \right) \hat{b}^\dagger \right] \Big|_{x,y=0} |0,0\rangle, \end{aligned} \quad (17)$$

which is the state of light at the output of the MZI. Based on Eq. (17), it is convenient to present the parity-based phase estimation scheme with calculations of its signal and phase sensitivity.

Parity detection is actually to perform photon number parity measurements on just one of the output modes of the MZI. The parity operator for the b mode can be expressed by^[44]

$$\hat{\Pi}_b = (-1)^{\hat{b}^\dagger \hat{b}} = \int \frac{d^2\gamma}{\pi} |\gamma\rangle \langle -\gamma|, \quad (18)$$

where $|\gamma\rangle$ is a coherent state. Thus, the expectation value of the parity operator in the output state is

$$\langle \hat{\Pi}_b(\varphi) \rangle = \text{MZI} \langle \text{out} | \int \frac{d^2\gamma}{\pi} |\gamma\rangle \langle -\gamma | \text{out} \rangle_{\text{MZI}}. \quad (19)$$

Different from the work in Ref. [19], now we directly calculate $\langle \hat{\Pi}_b(\varphi) \rangle$. Substituting Eq. (17) into Eq. (20), and applying the

integral formula^[45]

$$\int \frac{d^2z}{\pi} e^{\zeta|z|^2 + \xi z + \eta z^* + f z^2 + g z^{*2}} = \frac{e^{-\frac{\zeta \xi \eta + \xi^2 g + \eta^2 f}{\zeta^2 - 4fg}}}{\sqrt{\zeta^2 - 4fg}}, \quad (20)$$

whose convergent conditions are $\text{Re}(\zeta \pm f \pm g) < 0$ and $\text{Re}\left(\frac{\zeta^2 - 4fg}{\zeta \pm f \pm g}\right) < 0$, after performing straightforward calculation, we can obtain the signal of the parity detection as follows:

$$\begin{aligned} \langle \hat{\Pi}_b(\varphi) \rangle &= \langle \hat{\Pi}_b(\varphi) \rangle_0 \frac{\partial^{4n}}{(n!)^2 \partial x^n \partial y^n \partial t^n \partial \tau^n} \\ &\times \exp \left[\frac{(x^2 + t^2 - y^2 - \tau^2) \tanh r \sin(2\varphi)}{2 \cosh^2 r (1 - 2 \tanh^2 r \cos(2\varphi) + \tanh^4 r)} \right. \\ &- \frac{(xy + t\tau)(1 - \cos(2\varphi))(\tanh r + \tanh^3 r)}{1 - 2 \tanh^2 r \cos(2\varphi) + \tanh^4 r} \\ &+ \frac{(y\tau - xt) \sin \varphi \cosh(2r) \text{sech}^4 r}{1 - 2 \tanh^2 r \cos(2\varphi) + \tanh^4 r} \\ &\left. - \frac{(x\tau + yt) \cos \varphi \text{sech}^4 r}{1 - 2 \tanh^2 r \cos(2\varphi) + \tanh^4 r} \right] \Big|_{x,y,t,\tau=0}, \end{aligned} \quad (21)$$

where $\langle \hat{\Pi}_b(\varphi) \rangle_0$ is the signal of the parity detection when the TMSVS is considered as an input state of the MZI,

$$\langle \hat{\Pi}_b(\varphi) \rangle_0 = \frac{\text{sech}^2 r}{\sqrt{1 - 2 \tanh^2 r \cos(2\varphi) + \tanh^4 r}}, \quad (22)$$

which is just that result in Ref. [19] with $\bar{N} = 2 \sinh^2 r$. Following the work in Ref. [19], we have also made a shift transformation $\varphi \rightarrow \varphi + \pi/2$ in Eq. (21). Eq. (21) is the central result of this work, in what follows, it will be used to investigate the phase resolution and the phase sensitivity of the TMSTFS with the parity detection. Particularly, in the case of $r = 0$, we can obtain the signal of the parity detection with the twin-Fock state considered as the interferometer state, i.e.,

$$\begin{aligned} \langle \hat{\Pi}_b(\varphi) \rangle_{r=0} &= \frac{1}{(n!)^2} \frac{\partial^{4n}}{\partial x^n \partial y^n \partial t^n \partial \tau^n} \exp[(y\tau - xt) \sin \varphi \\ &- (x\tau + yt) \cos \varphi] \Big|_{x,y,t,\tau=0}, \end{aligned} \quad (23)$$

which is just the result in Ref. [46]. Equation (23) can be written in a simple form $\langle \hat{\Pi}_b(\varphi) \rangle_{r=0} = P_n(-\cos(2\varphi))$,^[13] where $P_n(x)$ is the Legendre polynomial. Based on Eq. (21), we draw Fig. 3 to show that the signal of the parity detection changes with the phase shift. For a given initial squeezing parameter r , Fig. 3(a) indicates that the central peak of $\hat{\Pi}_b(\varphi)$ at $\varphi = 0$ narrows when the values of n increases, which represents that the phase resolution can be enhanced in this scenario. However, if one gives the same total mean photon number, the TMSVS will exhibit the better phase resolution as shown in Fig. 3(b).

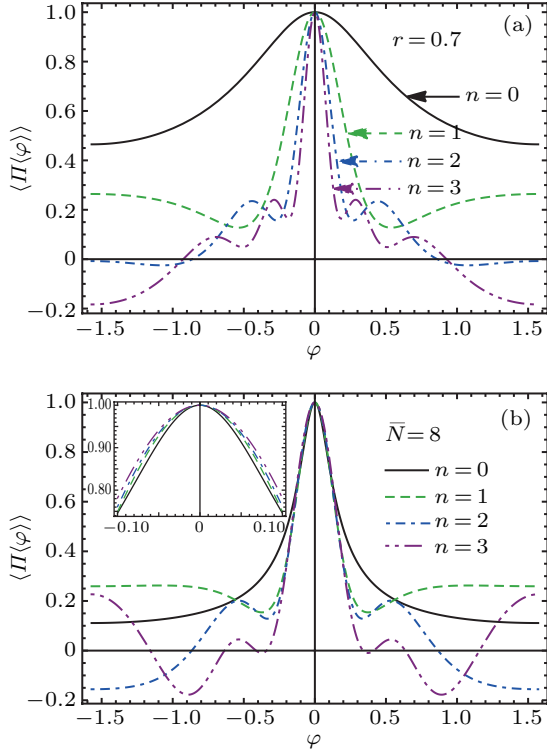


Fig. 3. Plots of the signal values of the parity detection against the phase shift: (a) for a given initial squeezing parameter, $r = 0.7$; (b) for a given total mean photon number, $\bar{N} = 8$.

4.2. Phase sensitivity of parity detection

Now we turn to investigate the phase sensitivity (or phase uncertainty) of the parity detection based on the classical Fisher information. For the parity detection, there are only two outcomes, e for even and o for odd. According to the concept, the classical Fisher information F_C for parity detection is given by^[36]

$$F_C = \frac{1}{P_e} \left(\frac{\partial P_e}{\partial \varphi} \right)^2 + \frac{1}{P_o} \left(\frac{\partial P_o}{\partial \varphi} \right)^2, \quad (24)$$

with the probabilities of even and odd counts

$$P_e = \frac{1}{2} (1 + \langle \hat{\Pi}(\varphi) \rangle), \quad P_o = \frac{1}{2} (1 - \langle \hat{\Pi}(\varphi) \rangle). \quad (25)$$

It is a difficult task to write out the explicit form of Eq. (24) for the TMSTFS with general values of n . However, in the case of $n = 0$, one can obtain the simple form of F_C as follows:

$$F_C|_{n=0} = \frac{\sinh^2(2r) \cos^2 \varphi}{(1 + \sinh^2(2r) \sin^2 \varphi)^2}. \quad (26)$$

From Eqs. (14) and (26), one can see clearly that the classical Fisher information achieves the quantum Fisher information in the case of $\varphi \rightarrow 0$. In addition, we also numerically realize that this is valid for general values of n . Therefore, the QCRB can be achieved in the limit $\varphi \rightarrow 0$ by parity detection. Substituting Eq. (25) into Eq. (24), and according to the classical Cramér–Rao bound, the phase sensitivity of parity detection is

bounded by

$$\Delta\varphi = \frac{1}{\sqrt{F_C}} = \frac{\sqrt{1 - \langle \hat{\Pi}(\varphi) \rangle^2}}{|\partial \hat{\Pi}(\varphi) / \partial \varphi|}. \quad (27)$$

In terms of the above calculations, we investigate the performance of the TMSTFS on the parity-based phase estimation scheme. Figure 4 shows that the phase sensitivity changes with the phase shift for some different values of n . For a given initial squeezing parameter r , one can see that the phase sensitivity at the optimal phase ($\varphi = 0$) can be enhanced by increasing the value of n . On the other hand, under energy constraint, we can see clearly that the TMSTFS provides a fairly constant phase sensitivity over a much broader range of accumulated phases as shown in Fig. 4(b). When the phase shift somewhat deviates from $\varphi = 0$, the TMSTFS can also offer the better phase sensitivity than the TMSVS for a given mean photon number. This is the second advantage of the TMSTFS for the phase estimation. Of course, under energy constraint, the TMSVS has the better phase sensitivity than the TMSTFS when the phase shift φ approaches to zero.

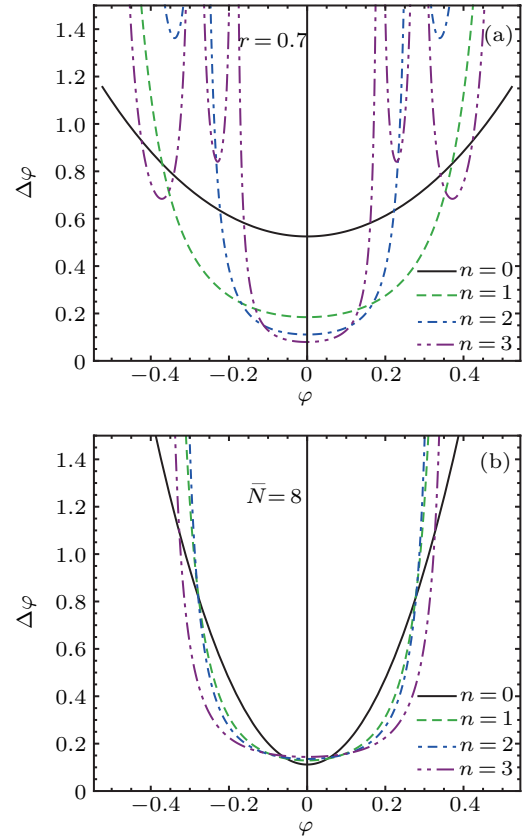


Fig. 4. Phase sensitivity $\Delta\varphi$ as a function of the phase shift φ for some different values of n : (a) for a given initial squeezing parameter, $r = 0.7$; (b) for a given total mean photon number, $\bar{N} = 8$.

In Fig. 5, we plot the phase sensitivity versus the initial squeezing parameter r at $\varphi = 10^{-3}$. Figure 5 shows that the phase sensitivity can be improved by increasing the value of n for any values of r . Under energy constraint, figure 6(a) indicates that the TMSVS gives the better phase sensitivity when

the phase shift approaches to zero. In addition, figure 6(a) shows that the difference among the phase sensitivity offered by the TMSTFS with different values of n is very small, especially for the large total mean photon number. However, when the phase shift slightly deviates from $\varphi = 0$, figure 6(b) indicates that the TMSTFS can still give the better phase sensitivity over a broad range of the total mean photon number where the uncertainty is still below the SNL, which is also consistent with Fig. 4(b).

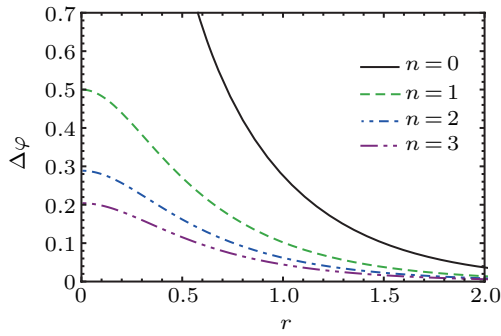


Fig. 5. Phase sensitivity $\Delta\varphi$ as a function of the initial squeezing parameter r for different values of n at $\varphi = 10^{-3}$.

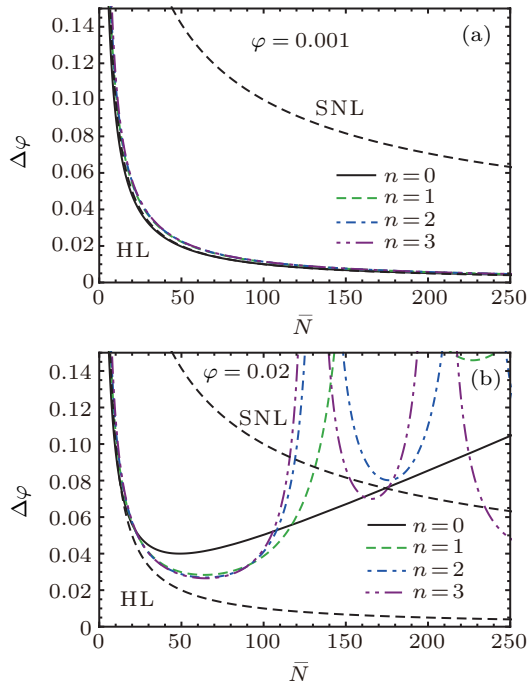


Fig. 6. Phase sensitivity $\Delta\varphi$ as a function of the total mean photon number for different values of n : (a) $\varphi = 10^{-3}$, (b) $\varphi = 0.02$.

5. Conclusions

In this work, we have investigated theoretically the performance of the TMSTFS on the quantum enhanced metrology. Via parity detection and quantum Fisher information, our results show that, compared with the TMSVS, both phase resolution and phase sensitivity can be enhanced by the TMSTFS for a given initial squeezing parameter. On the other hand, within a constraint on the total photon number, the TMSVS

gives the better QCRB. These results are similar to the properties of the quantum entanglement of the TMSTFS. However, via parity detection, the phase sensitivity offered by the TMSVS will rapidly becomes worse, even above the SNL, when the phase shift moderately deviates from $\varphi = 0$. This is in marked contrast to what happens for the TMSTFS, which are relatively stable in that sense. That is to say, when the phase shift slightly deviates from zero, the TMSTFS can give the better phase sensitivity over a broad range of the total photon number where the phase uncertainty is still below the SNL, even under energy constraint. Therefore, compared with the TMSVS, the phase sensitivity can be indeed enhanced by the TMSTFS on some different occasions. These results are useful towards a complete understanding of quantum non-Gaussian states for quantum informatics. Finally, we show that the QCRB can be approached via the parity detection for the TMSTFS when the phase shift comes nearly to zero.

References

- [1] Yurke B, McCall S L and Klauder J R 1986 *Phys. Rev. A* **33** 4033
- [2] Caves C M 1981 *Phys. Rev. D* **23** 1693
- [3] Wei C P, Hu X Y and Zhang Z M 2016 *Chin. Phys. B* **25** 040601
- [4] Guo L L, Yu Y F and Zhang Z M 2018 *Opt. Express*, **26** 29099
- [5] Pezzè L and Smerzi A 2008 *Phys. Rev. Lett.* **100** 073601
- [6] Seshadreesan K P, Anisimov P M, Lee H and Dowling J P 2011 *New J. Phys.* **13** 083026
- [7] Holland M J and Burnett K 1993 *Phys. Rev. Lett.* **71** 1355
- [8] Ou Z Y 1996 *Phys. Rev. Lett.* **77** 2352
- [9] Lee H, Kok P and Dowling J P 2002 *J. Mod. Opt.* **49** 2325
- [10] Dowling J P 2008 *Contemp. Phys.* **49** 125
- [11] Rubin M A and Kaushik S 2007 *Phys. Rev. A* **75** 053805
- [12] Jiang K, Brignac C J, Weng Y, Kim M B, Lee H and Dowling J P 2012 *Phys. Rev. A* **86** 013826
- [13] Campos R A, Gerry C C and Benmoussa A 2003 *Phys. Rev. A* **68** 023810
- [14] Sun F W, Liu B H, Gong Y X, Huang Y F, Ou Z Y and Guo G C 2008 *Europhys. Lett.* **82** 24001
- [15] Xiang G Y, Higgins B L, Berry D W, Wiseman H M and Pryde G J 2011 *Nat. Photon.* **5** 43
- [16] Xiang G Y, Hofmann H F and Pryde G J 2013 *Sci. Rep.* **3** 2684
- [17] Jin R B, Fujiwara M, Shimizu R, Collins R J, Buller G S, Yamashita T, Miki S, Terai H, Takeoka M and Sasaki M 2016 *Sci. Rep.* **6** 36914
- [18] Wei C P and Zhang Z M 2017 *J. Mod. Opt.* **64** 743
- [19] Anisimov P M, Raterman G M, Chiruvelli A, Plick W N, Huer S D, Lee H and Dowling J P 2010 *Phys. Rev. Lett.* **104** 103602
- [20] Eberle T, Händchen V and Schnabel R 2013 *Opt. Express* **21** 11546
- [21] Gerry C C and Mimih J 2010 *Phys. Rev. A* **82** 013831
- [22] Carranza R and Gerry C C 2012 *J. Opt. Soc. Am. B* **29** 2581
- [23] Hou L L, Xue J Z, Sui Y X and Wang S 2019 *Chin. Phys. B* **28** 094217
- [24] Ouyang Y, Wang S and Zhan L J 2016 *J. Opt. Soc. Am. B* **33** 1373
- [25] Chizhov A V and Murzakhmetov B K 1993 *Phys. Lett. A* **176** 33
- [26] Dell'Anno F, De Siena S and Illuminati F 2006 *Open Sys. Inform.* **13** 383
- [27] Namiki R 2010 *J. Phys. Soc. Jpn.* **79** 013001
- [28] Xiang S, Zhu X and Song K 2018 *Chin. Phys. B* **27** 100305
- [29] Hu L Y and Fan H Y 2008 *Commun. Theor. Phys.* **50** 965
- [30] Tilma T, Hamaji S, Munro W J and Nemoto K 2010 *Phys. Rev. A* **81** 022108
- [31] Braun D, Adesso G, Benatti F, Floreanini R, Marzolino U, Mitchell M W and Pirandola S 2018 *Rev. Mod. Phys.* **90** 035006
- [32] Pezzè L and Smerzi A 2018 *Rev. Mod. Phys.* **90** 035005
- [33] Bennett C H, Bernstein H J, Popescu S and Schumacher B 1996 *Phys. Rev. A* **53** 2046

- [34] Helstrom C W 1976 *Quantum detection and estimation theory* (New York: Academic Press)
- [35] Ben-Aryeh Y 2012 *J. Opt. Soc. Am. B* **29** 2754
- [36] Seshadreesan K P, Kim S, Dowling J P and Lee H 2013 *Phys. Rev. A* **87** 043833
- [37] Li D, Yuan C H, Ou Z Y and Zhang W P 2014 *New J. Phys.* **16** 073020
- [38] Oh C, Lee S Y, Nha H and Jeong H 2017 *Phys. Rev. A* **96** 062304
- [39] Anderson B E, Gupta P, Schmittberger B L, Horrom T, Hermann-Avigliano C, Jones K M and Lett P D 2017 *Optica* **4** 752
- [40] Plick W N, Dowling J P and Agarwal G S 2010 *New J. Phys.* **12** 083014
- [41] Marino A M, Corzo Trejo N V and Lett P D 2012 *Phys. Rev. A* **86** 023844
- [42] Szigeti S S, Lewis-Swan R J and Haine S A 2017 *Phys. Rev. Lett.* **118** 150401
- [43] Anderson B E, Schmittberger B L, Gupta P, Jones K M and Lett P D 2017 *Phys. Rev. A* **95** 063843
- [44] Fan H Y and Ruan T N 1983 *Commun. Theor. Phys.* **2** 1563
- [45] Puri R R 2001 *Mathematical methods of quantum optics* (Berlin: Springer-Verlag), Appendix A
- [46] Wang S, Wang Y T, Zhai L J and Zhang L J 2018 *J. Opt. Soc. Am. B* **35** 1046